

Application of AC-SECM in Corrosion Science: Local Visualization of Heterogeneous Chemical Activity in AA2024 Surfaces

Javier Izquierdo, Sergio González, Ricardo M. Souto*

Department of Physical Chemistry, University of La Laguna, E-38200 La Laguna (Tenerife), Spain

*E-mail: rsouto@ull.es

Received: 5 October 2012 / Accepted: 20 October 2012 / Published: 1 November 2012

Aluminium alloy AA2024-T3 surfaces have been characterised by using a new microelectrochemical technique, frequency-dependent alternating current scanning electrochemical microscopy (AC-SECM), which does not require the addition of any redox active species to the electrolyte solution. Information regarding the topography and/or redox activity of the solid/liquid interface is obtained in situ, allowing their evolution with time to be monitored with high spatial resolution. By scanning the microelectrode over the surface, an image is generated, as well as information concerning reactions that take place in the solution space between the tip and the sample or on the surface of the scanned sample. A heterogeneous response due to the presence of intermetallic inclusions precipitated in the material is found on AA2024-T3 surfaces. The highly localized anodic activity was thus detected, which has been interpreted as a result of the galvanic coupling between the matrix and the intermetallic particles.

Keywords: AA2024, SECM, AC-SECM, aluminium alloy, intermetallic particles, localized corrosion.

1. INTRODUCTION

Despite its considerably low standard reduction potential, aluminium is relatively resistant towards corrosion thanks to the passive layer formed on its surface [1-7]. In order to improve the mechanical properties of the metal for industrial applications, it becomes necessary to alloy it with other metals. In this way, alloy series AA2xxx and AA7xxx have found extensive use in several engineering and scientific applications, especially in the aerospace industries, because they exhibit high strength-to-weight ratios [7,8]. Improvement of the mechanical properties is achieved through the precipitation of metallic inclusions during optimized thermal treatments for each specific material. However, these particles, with different composition than the matrix, may promote galvanic coupling

and subsequent highly localized corrosion [8-13], which is a major problem affecting other technological materials such as steels containing MnS precipitates [14-16].

During the corrosion process, local microcells are developed on the metal exposed to an aggressive electrolyte. These microanodes and microcathodes are distributed over the metallic surface due to different asymmetries existing in the material. At the anodic sites, evolution of metal cations and degradation of the material takes place by oxidation (1). This dissolution, when the substrate is an alloy, is more likely to be selective, with the most active elements being oxidized first. Electrons produced in this half-reaction flow to the cathodic sites, participating in the reduction of the oxidant, a role that, depending on the media, may be assumed by oxygen in aerated electrolytes at neutral and alkaline pH (2), or by protons at lower pH and/or poorly oxygenated solutions (3) [17]:



In particular, the AA2024 alloy presents two main types of precipitates that compromise its corrosive susceptibility: Mg-rich particles or s-phase particles, with composition Al(MgCu), that behave anodic with respect to the matrix, and Cu-rich particles, with composition Al(CuMnFe), that, in contrast, behave cathodic [7,9,10,18-24]. The former are usually smaller than 5 μm diameter and selectively dissolve Mg, subsequently acting as cathodes, and promoting degradation of the surrounding matrix until they are released when no matrix sustains them. Concerning the Cu-rich ones, they are also released after enough time of attack to the proximal matrix, but its usual greater size (ca. 20-50 μm diameter), helps them to be retained for longer times. These phenomena have consequences in both topography and surface activity, and some aspects of the corrosion mechanism are still under discussion.

Conventional electrochemical methods for corrosion research, such as polarization or electrochemical impedance, gain information regarding electrochemical reactions taking place on the metal-electrolyte interface. However, they only provide the average results of the whole surface under study, and lack the spatial resolution that would allow the proper analysis of the heterogeneity of samples responsible for their localized attack.

Chemical imaging of surfaces has been achieved with the development of scanning electrochemical microscopy (SECM) [25-27]. SECM is based on the reaction that occurs at a mobile ultramicroelectrode probe (UME) immersed in an electrolyte solution, and accurately rastered in close vicinity of a substrate surface in order to characterize the topography and/or redox activity of the solid/liquid interface. Measurements are performed recording electrochemical signals related to the interaction with the surface of a redox species in the solution phase [25,26]. Electrochemical operation is usually amperometric, applying a potential to the UME, and recording the current at the probe as the

measuring signal. When a diffusion-controlled reversible redox reaction is used as electrochemical mediator, the faradaic current measured at the tip is affected by the nature of the surface under investigation and the tip-substrate distance. The surface may either block its diffusion towards the tip, or may facilitate a reaction site for it (i.e. being produced, consumed, etc). Separate control of the electric state of the substrate can be attained by using a bipotentiostat as electrochemical interface in the system, allowing for the controlled polarization of the sample. Nevertheless, operation of the system under open circuit conditions is of a great advantage, especially when naturally corroding conditions are explored. Unfortunately, the need of a redox mediator in solution may affect the electrical state of the surface, because the electrochemical mediator can polarize the system. That is, the potential of the system is determined by the ratio between the two species involved in the redox couple, and can be determined by applying the Nernst equation [28]. Additionally, the possible interference of any of the redox species on the actual corrosion process under investigation cannot be discarded, particularly when thin surface films, such as those formed during the adsorption of corrosion inhibitors on metals, are involved [29].

This limitation of scanning electrochemical microscopy can be overcome by using a different technique, frequency-dependent alternating current scanning electrochemical microscopy (AC-SECM) [28]. In this case, an oscillating potential perturbation is applied to the tip, and the AC current flowing at the tip is measured for different frequencies of the perturbation signal [28,30]. This feature strongly amplifies the possibilities of the SECM, since results will also be conditioned by the parameters of the voltage oscillation whereas it does not require the addition of electrochemical mediators. It has been demonstrated that the alternating current response may be successfully used to monitor variations in the local chemical activity of a surface [30]. The applicability of this technique in corrosion science has already been found in the detection of corrosion pits [31,32], the monitoring of metal release [33,34], the imaging of the early stages of blistering under an organic coating applied on a metal [35], and the local visualisation of inhibitor films on active metals for corrosion protection [36,37]. At this stage, it was considered that a new application of technological interest might be found in the visualization of chemical heterogeneities in reactive materials such as aluminium alloys.

2. EXPERIMENTAL

2.1. Samples and solutions

Measurements were performed on AA 2024-T3 substrates of composition given in Table 1. The surface of the samples was abraded with SiC paper up to grit 4000. The resulting surfaces were degreased with acetone, abundantly rinsed with ultra-pure deionised water and allowed to dry in air. They were mounted facing up in the electrochemical cell, and immersed in NaCl solutions as test media. Ferrocene-methanol (Aldrich) was added as redox mediator when necessary in SECM experiments. All solutions were prepared with analytical grade reagents and ultra-pure water purified with a Milli-Q system from Millipore.

Table 1. Composition of AA 2024 aluminium alloy (wt.%)

Al	Balance
Cu	3.8 - 4.9
Mg	1.2 - 1.8
Si	< 0.5
Fe	< 0.5
Mn	0.3 - 0.9
Zr	< 0.25
Ti	< 0.15
Cr	< 0.1

2.2. Electrodes and instrumentation

The set-up for electrochemical measurements consisted on a Teflon cell with a circular orifice of 5 mm diameter at its bottom to facilitate the exposure of the sample to the test environment. Around 2 ml of solution was added in each case as electrolytic medium. A video microscope was used to aid microelectrode positioning and sample levelling using three thumbscrews arranged in a tripod configuration. An Ag/AgCl/KCl (3M) reference electrode, and a stainless steel wire used as counter electrode were also introduced in the electrochemical microcell.

SECM measurements were carried out with a microscope built by Sensolytics (Bochum, Germany). A three electrode configuration was employed, with 10 μm Pt microelectrode as working electrode, stainless steel as auxiliary-electrode and Ag/AgCl/KCl (3M) as reference. All potentials mentioned in this work are referred to this electrode. Amperometric SECM measurements were carried out applying a constant potential of +0.50 V in 0.50 mM ferrocene-methanol solution, ensuring oxidation of this species on the tip under diffusion control. 2-D motion was performed parallel to the surface of the substrate at 15 μm tip-substrate height.

For AC-SECM measurements, an EG&G Princeton Applied Research potentiostat (Princeton, NJ, USA), model 273A was connected to the SECM equipment, whereas measurement of the AC current was performed using the lock-in amplifier available in the instrument for the high resolution operation. The same ultramicroelectrodes than in conventional SECM were employed for the alternating current operation. Data acquisition involved at least 4 dimensions, namely the 2-D related to the position in the XY plane in which the scan is recorded, AC current data and frequency. AC voltage signals of 10 mV_{pp} amplitude were applied around a constant base potential for 10 frequency values in 60000 Hz to 1000 Hz range. The constant potential value was either +0.50 V when ferrocene-methanol was added to the test electrolyte, or the open circuit potential (OCP) developed spontaneously in the solution. Measurements were performed in 1 mM NaCl.

3. RESULTS AND DISCUSSION

3.1. SECM characterization

In a first series of experiments, the establishment of a correlation between the results obtained using conventional amperometric operation of SECM, and those delivered by the new alternating-current mode, was attempted. In order to locate the surface, the tip was progressively moved towards the surface and experimental approach curves were measured in a solution containing ferrocene-methanol. The corresponding plots for the two operation modes are shown in Figure 1. In both cases, the current signals measured at the tip have been normalized by dividing the values at each tip-substrate distance by the corresponding value measured in the bulk of the solution, i_{lim} and MAG respectively.

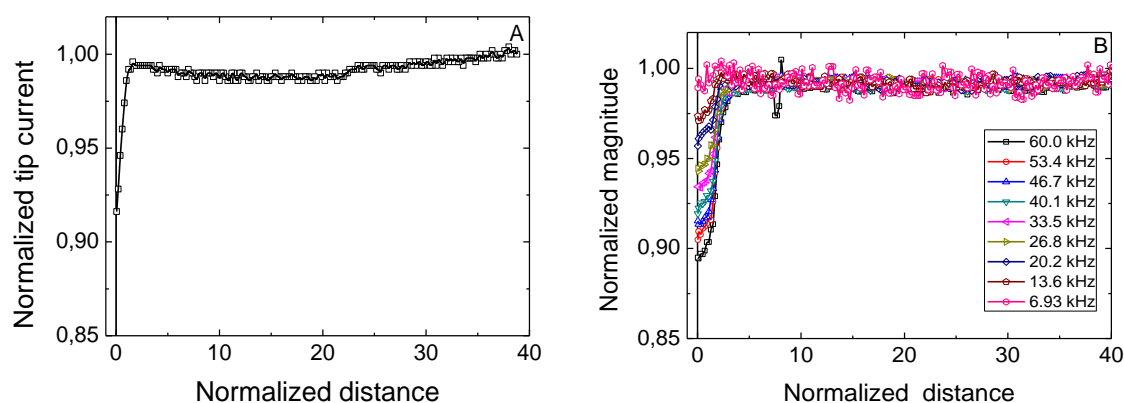


Figure 1. Normalized change in the current measured at the tip electrode as a function of distance from the AA2024 bare surface (i.e., approach curves). The SECM operation was: (A) amperometric, and (B) alternating-current modes. Test environment: 0.5 mM ferrocene-methanol. DC potential: +0.50 V vs. Ag/AgCl/KCl (3M). Amplitude of the AC potential signal: 10 mV_{pp} for the frequencies indicated in the legend. Tip diameter: 10 μm. The non dimensional tip-to-substrate distance is given by d/a , where d is the actual distance, and a the diameter of the Pt microelectrode.

A negative feedback effect is observed when applying a constant potential in Figure 1A, leading to a sudden decrease in current when the diffusion of the redox mediator towards the tip is hindered by the close proximity of the substrate. However, a small increase in current can be observed just before this decay, which probably arises from the partial reduction at the substrate of some ferrocinium ions produced during the oxidation of ferrocene-methanol at the UME. In this way, greater concentrations of the electroactive species are encountered at small tip-to-substrate distances. Thus, a combined situation of positive and negative feedback is observed, indicating that this surface is active enough to allow some redox regeneration of the mediator, though the kinetics of this electronic exchange is not fast enough to overcome the limitation to diffusion imposed at small distances. This result can be justified considering that aluminium alloys are known to form a passive layer with lower conductivity than the metal, effectively slowing the rate of the electronic exchange reaction [17].

After completing the measurement of the approach curve under amperometric SECM operation, the same procedure was followed to measure a new approach curve above the same location of the surface, but under AC operation of the SECM. The corresponding approach curves for a selection of frequencies of the AC signal are given in Figure 1B. There exists a decrease in the value of the magnitude of the AC current when the tip approximates the substrate, which is consistent with the greater resistance offered by the small volume of electrolyte available for ionic conduction. This response is more pronounced at higher frequencies, whereas at 6.93 kHz the proximity of the surface is hardly noticeable. In the figure, the corresponding plot for 1.00 kHz has been omitted as the surface could not be distinguished at this frequency.

In the case of a metallic substrate, when the electrolyte concentration is low, the equivalent circuit that better fits to the system is depicted in Figure 2 and can be described as it follows [28]. When the tip is far enough from the surface, electric motion takes place through the electrolyte and the only term altering the obtained signal is the solution resistance. If the tip approaches the metal surface, electric charges find another alternative route through the substrate, now affecting the resistance and the capacitance at the metal-substrate interface, especially at the local position of the tip. In addition, electric motion in solution is reduced due to the blockage of diffusion. As a result, by approaching the UME to the sample, the impedance of the system will be altered, thus affecting the modulus and phase angle of the AC current, and this will be strongly dependent on the frequency. Conversely, on the tip approaching an insulator surface, a thinner electrolyte layer of the solution is left between the tip and the substrate, so the solution resistance increases and the current drops.

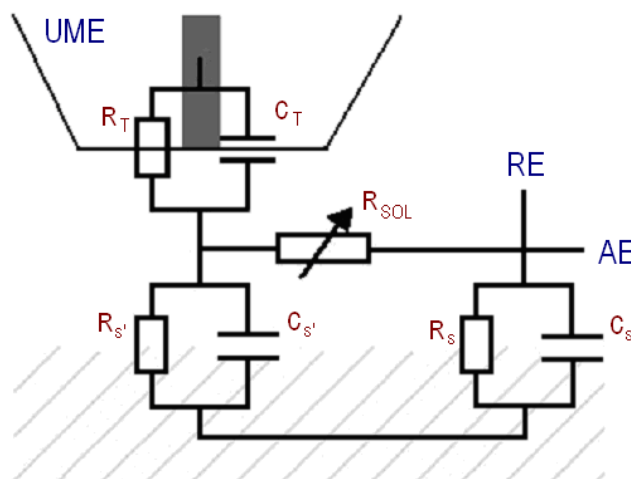


Figure 2. Equivalent circuit representing the impedance behavior of the metal/electrolyte system [28]: R_T and C_T are resistance and capacitance of the tip, respectively; R_{SOL} is the solution resistance; R_S and C_S are the resistance and capacitance of the sample, being $R_{S'}$ and $C_{S'}$ these parameters at the specific area covered by the AC-SECM tip.

Therefore, inspection of Figure 1B indicates that the substrate behaves as an insulator at the highest frequency under consideration, thus the AC-SECM response is solely determined by the tip-substrate distance. In this way, topographic information is obtained exclusively. A sufficiently high

frequency value should be found that provides the greatest contrast for topographic imaging. On the other hand, it is also observed that the current measured at the distance of closest approach progressively grows with the decrease in the applied frequency. That is, the chemical characteristics of the surface affect the current response measured at the tip in the low frequency range of the AC signal. Local differences in chemical reactivity occurring in the investigated surface should be spatially resolved at lower frequency values.

In order to image the chemical heterogeneity of the surface under study, scans measured at constant height were recorded under the same experimental conditions employed in Figure 1, and the resulting maps are depicted in Figure 3. The SECM image in Figure 3A, obtained with amperometric SECM, exhibits some areas with higher tip current values. They correspond to locations at which faster regeneration of the mediator occurs, a feature previously reported in the scientific literature [40,41]. These zones, assumed to correspond to intermetallic particles, present greater electronic exchange with species from the solution. This ability is generally due to either a less insulating passive layer that makes the specimen more electrically conductive, and/or different surface potential that facilitates the donation of electrons to the ferrocinium ion. However, the later would contradict the observations of scanning Kelvin probe force microscopy [20,32,34]. According to them, intermetallics that may be more easily observed thanks to their size and persistence on the surface are the Al(CuMnFe) ones, with nobler potential, so they are not so likely to donate electrons, and the hypothesis of the thinner passive layer above these particles seems to more adequately describe the observed results.

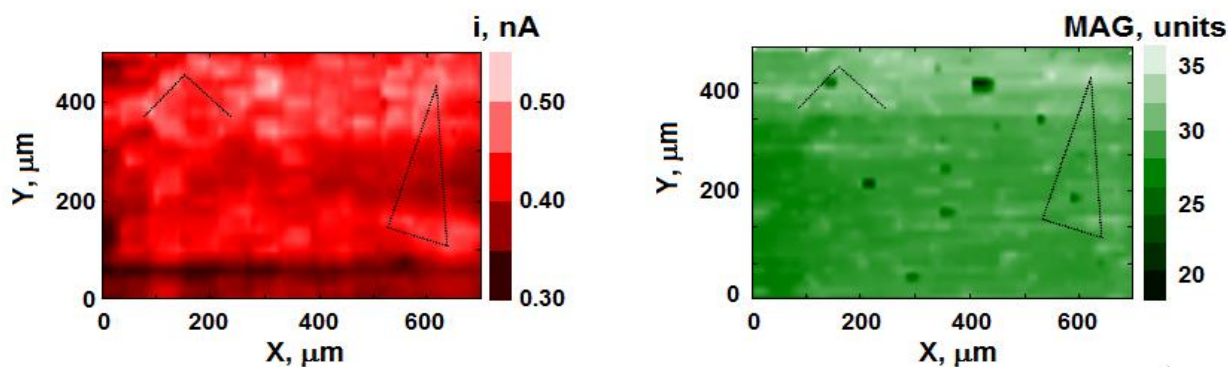


Figure 3. SECM images obtained over an AA 2024 bare surface immersed in 0.5 mM ferrocene-methanol solution. The SECM operation was: (left) amperometric, and (right) alternating-current modes. DC potential: +0.50 V vs. Ag/AgCl/KCl (3M). Amplitude of the AC potential signal: 10 mV_{pp}, and frequency of 33.5 kHz. Tip diameter: 10 μm; tip-substrate distance: 15 μm.

After recording a map with conventional SECM, the same area of the surface was monitored employing the alternating-current mode of SECM, and the image shown in Figure 3B was recorded. The image was obtained at the frequency of 33.5 kHz, which provided the greater contrast. It can be observed that certain active sites already detected using the conventional operation (cf. marks in the figure), are also seen in the AC-SECM map as regions of enhanced current modulus. Furthermore, the features occurring in the surface are resolved with greater sensitivity in the alternating current image.

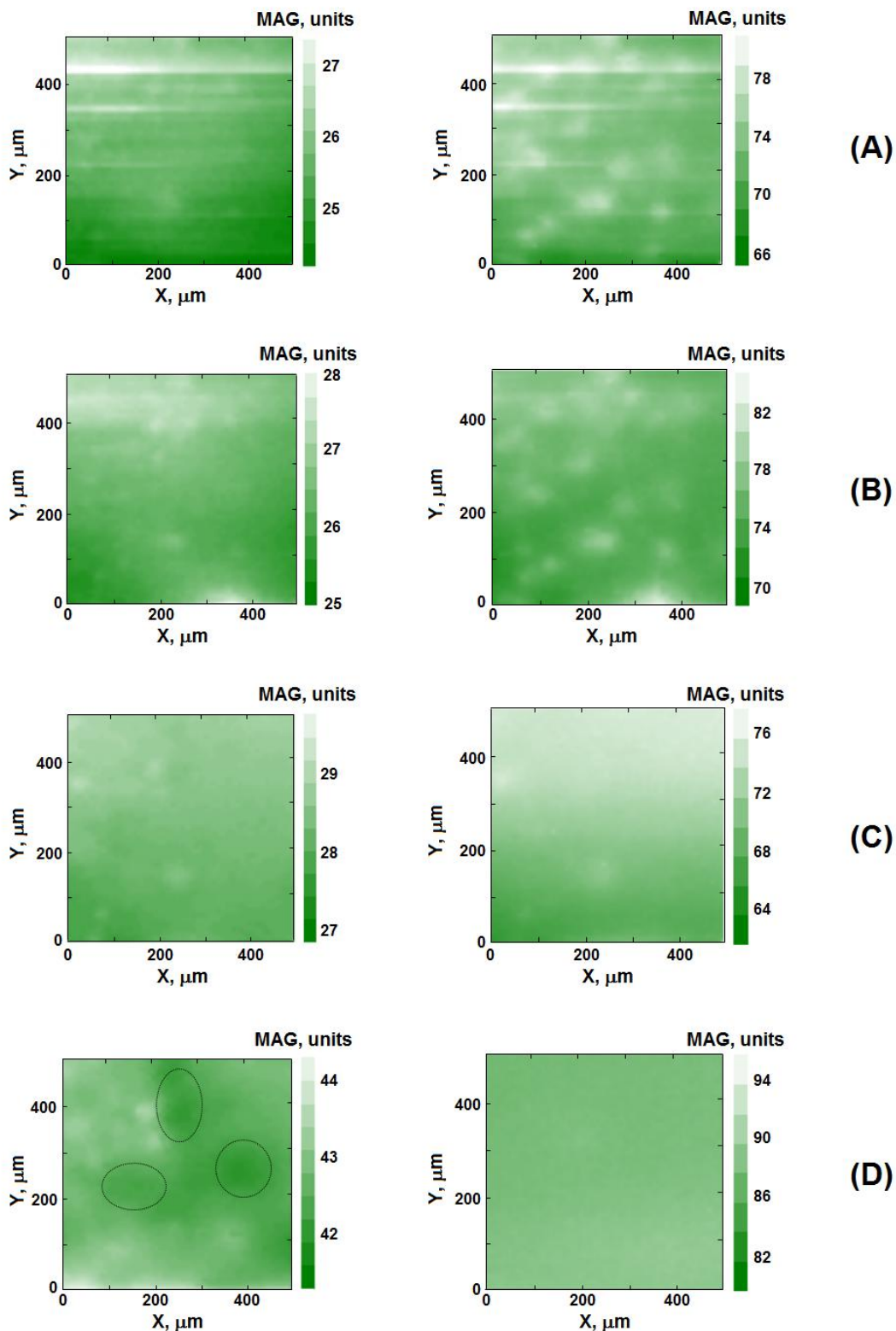


Figure 4. Change in the modulus of the tip AC current observed while scanning over an AA 2024 bare surface immersed in 10 mM NaCl after: (A) 60 min, (B) 105 min, (C) 255 min, and (D) 17 hours immersion. Tip diameter: 10 μm ; tip-substrate distance: 15 μm . Amplitude of the AC potential signal: 10 mV_{pp} . Frequency was: (left) 55.0 kHz, and (right) 6.93 kHz.

At this stage, it must be taken in account that these preliminary experiments were performed adding a redox mediator to the solution for imaging with conventional SECM, and this procedure may produce some drawbacks during measurements. Firstly, we cannot ensure that the mediator is not affecting the spontaneous evolution of the substrate, and there is no special application in studying the influence of ferrocene-methanol on these substrates as for real systems. Secondly, the tip showed a stable trend to produce decreasing currents when biased at +0.50 V in this solution, as if it was becoming progressively blocked either by some chemical species originating from the active metal and subsequently reacting at the microelectrode, or as if ferrocene-methanol concentration was effectively decreasing with time due by reaction of this species with the metal sample (i.e. being oxidized by oxygen present in the naturally aerated solution acting the metal as a catalyst). Therefore, we decided to analyze a new sample in a mediator-free solution, and in the presence of a more aggressive media. For that purpose, AC-SECM scans were performed in 1 mM NaCl solutions. Figures 4 and 5 show the AC-SECM images of an AA2024 sample immersed in 10 mM NaCl for different exposures, as registered at two different frequencies, namely 55 and 7 kHz. They are given as both the modulus and phase angle components of the AC current flowing in the system. The images of the current modulus imaged for different durations of the immersion in the electrolytic media shows an almost homogeneous surface at the early stages of the experiment (cf. Fig. 4).

However, the longer the time they are exposed to the electrolyte, the activation of specific sites in the surface are observed as regions of increased current modulus in the plots. This chemical activation effect is viewed in the development of small regions that appear lighter in the image recorded at the frequency of 55 kHz, which actually corresponds to higher current modulus values. That is, these areas are effectively located at a bigger distance from the tip than the surrounding surface when the tip scans over the sample at a constant height. Therefore, the development of holes in the surface has been imaged, which according to our observations might correspond with the loose of the matrix material surrounding cathodic intermetallic particles. This observation agree with reports in the literature based on ex situ analysis by scanning electron microscopy [10,18-24]. Additionally, the higher current modulus values recorded over the whole imaged surface at both frequency values after the sample has been exposed to the solution overnight, is an indication that the aged oxide layer is less insulating than at earlier exposures. The absence of features in the image taken in Figure 4D at the lower frequency of 6.93 kHz, supports that all the surface is covered likewise by this film. Yet, the different physicochemical properties of the surface oxide film is evidenced from the comparison of the current phase images for these two frequency values given in Figure 5. Though they appear rather featureless at both frequency values, especially in the case of the longer exposures of the sample in the electrolyte solution, it is directly observable that low phase values are only observed in Figure 5D with the frequency of 6.93 kHz. This value corresponds to a resistive system, whereas higher phase values are more consistent with a dielectric barrier film displaying a somewhat capacitive behaviour towards the passage of AC current. Again the physicochemical characteristics of the surface have been viewed from the AC-SECM images taken at the lowest frequency, whereas the phase values are always high and almost invariable throughout the duration of the experiments in the images taken with the frequency of 55 kHz.

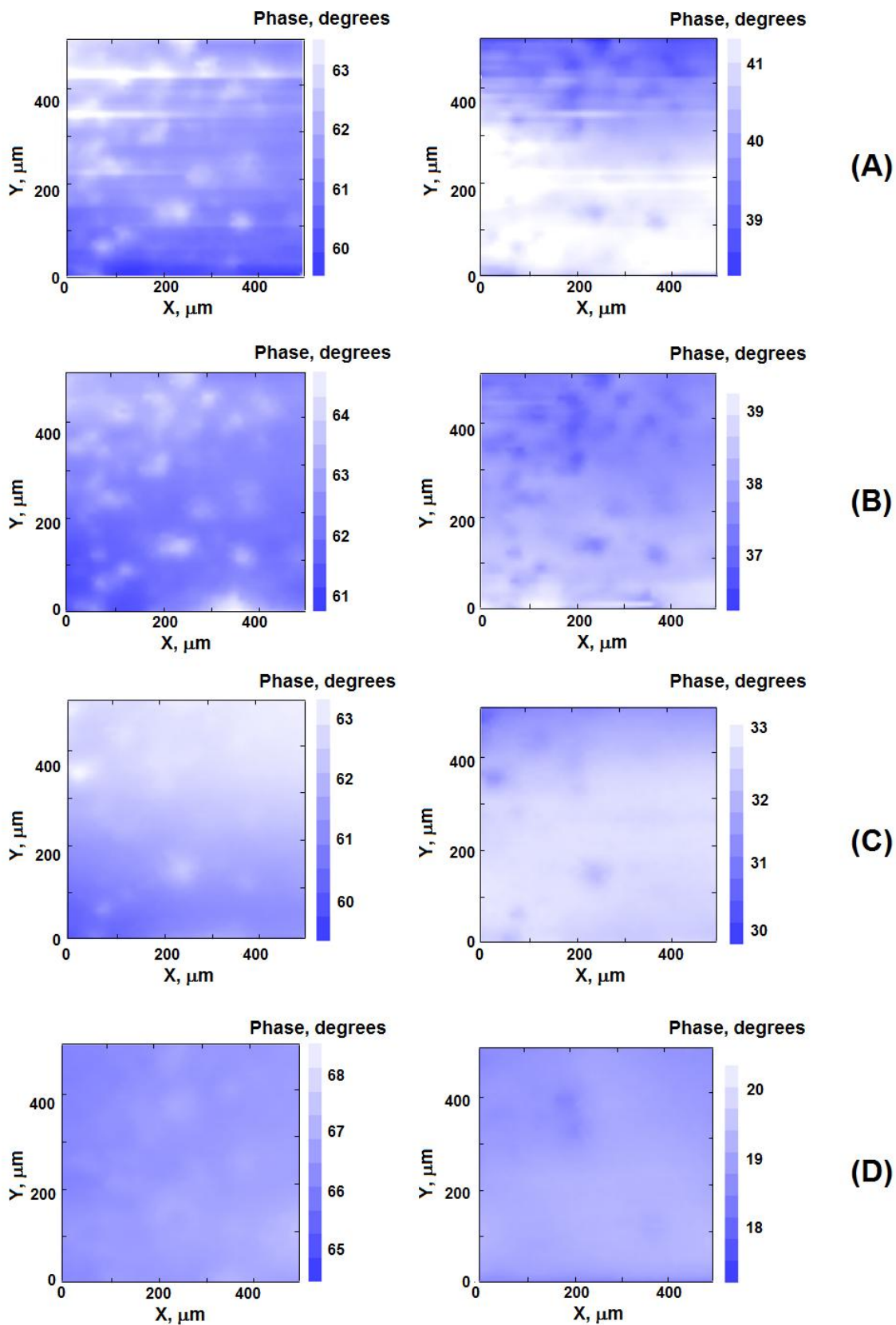


Figure 5. Change in the phase of the tip AC current observed while scanning over an AA 2024 bare surface immersed in 10 mM NaCl after: (A) 60 min, (B) 105 min, (C) 255 min, and (D) 17 hours immersion. Tip diameter: 10 μm ; tip-substrate distance: 15 μm . Amplitude of the AC potential signal: 10 mV_{pp}. Frequency was: (left) 55.0 kHz, and (right) 6.93 kHz.

4. CONCLUSION

The application of a new technique, alternating-current scanning electrochemical microscopy (AC-SECM), to the characterization of the electrochemical behaviour of AA 2024 exposed to a dilute aqueous solution containing NaCl has provided new insights towards the elucidation of the surface processes related to the corrosion of this material. Spatially-resolved images combining topographic and chemical activity information could be obtained by adequately tuning the frequency of the AC current used as measuring signal. Local activation of inclusions and dissolution processes related to their electrochemical activity could be monitored both topographically and chemically. The evolution of physicochemical characteristics of the surface films spontaneously formed on the material during immersion in the electrolyte as a function of time could be determined as changes in its resistance to undergo charge transfer reactions through these layers.

ACKNOWLEDGMENTS

The authors are grateful for financial support by the Spanish Ministry of Science and Innovation (MICINN, Madrid) and the European Regional Development Fund (Brussels, Belgium) under Project No. CTQ2009-12459. A Research Training Grant awarded to J.I. by the Spanish Ministry of Education (Programa de Formación de Personal Investigador) is gratefully acknowledged.

References

1. C.A. Melendres, S. van Gils, H. Terryn, *Electrochem. Commun.* 3 (2001) 737.
2. J.C.S. Fernandes, R. Picciochi, M. da Cunha Belo, T.M. Silva, M.G.S. Ferreira, I.T.E. Fonseca, *Electrochim. Acta* 49 (2004) 4701.
3. F.J. Martin, G.T. Cheek, W.E. O'Grady, P.M. Natishan, *Corros. Sci.* 47 (2005) 3187.
4. J. Bernard, M. Chatenet, F. Dalard, *Electrochim. Acta* 52 (2006) 86.
5. M.A. Amin, S.S. Abd El Rehim, E.E.F. El Sherbini, *Electrochim. Acta* 51 (2006) 4754.
6. D. Battistel, S. Daniele, G. Battaglin, M.A. Baldo, *Electrochem. Commun.* 11 (2009) 2195.
7. J. Zhang, M. Klasky, B.C. Letellier, *J. Nuclear Mater.* 384 (2009) 175.
8. M. Morozov, G.Y. Tian, P.J. Withers, *DT&E International* 43 (2010) 493.
9. P. Campestrini, E.P.M. van Westing, H.W. van Rooijen, J.H.W. de Wit, *Corros. Sci.* 42 (2000) 1853.
10. P. Campestrini, H.W. van Rooijen, E.P.M. van Westing, J.H.W. de Wit, *Mater. Corros.* 51 (2000) 616.
11. B.A. Shaw, R.G. Buchheit, J. P. Moran (Eds.), *Corrosion and corrosion prevention of low density metals and alloys*. The Electrochemical Society, Pennington, NJ, (2001).
12. F. Andreatta, M.M. Lohrengel, H. Terryn, J.H.W. de Wit, *Electrochim. Acta* 48 (2003) 3239.
13. F. Andreatta, H. Terryn, J.H.W. de Wit, *Electrochim. Acta* 49 (2004) 2851.
14. C.H. Paik, H.S. White, R.C. Alkire, *J. Electrochem. Soc.* 147 (2000) 4120.
15. V. Vignal, H. Krawiec, O. Heintz, R. Oltra, *Electrochim. Acta* 52 (2007) 4994.
16. F. Zhang, J. Pan, C. Lin, *Corros. Sci.* 51 (2009) 2130.
17. D.A. Jones, *Principles and prevention of corrosion*. Maxwell Macmillan International Editions, New York (1992).
18. R.G. Buchheit, R.P. Grant, P.F. Hiava, B. Mckenzie, G.L. Zende, *J. Electrochem. Soc.* 144 (1997) 2621.
19. R.P. Wei, C.-M. Liao, M. Gao, *Metall. Mater. Trans. A* 29 (1998) 1153.

20. T. Suter, R.C. Alkire, *J. Electrochem. Soc.* 148 (2001) B36.
21. K.A. Yasakau, M.L. Zheludkevich, S.V. Lamaka, M.G.S. Ferreira, *J. Phys. Chem. B* 110 (2006) 5515.
22. F.M. Queiroz, M. Magnani, I. Costa, H.G. de Melo, *Corros. Sci.* 50 (2008) 2646.
23. A. Boag, A.E. Hughes, A.M. Glenn, T.H. Muster, D. McCulloch, *Corros. Sci.* 53 (2011) 17.
24. A.E. Hughes, A. Boag, A.M. Glenn, D. McCulloch, T.H. Muster, C. Ryan, C. Luo, X. Zhou, G.E. Thompson, *Corros. Sci.* 53 (2011) 27.
25. A.J. Bard, F.-R.F. Fan, J. Kwak, O. Lev, *Anal. Chem.* 61 (1989) 132.
26. J. Kwak, A.J. Bard, *Anal. Chem.* 61 (1989) 1221.
27. A.J. Bard, G. Denuault, C. Lee, D. Mandler, D.O. Wipf, *Acc. Chem. Res.* 23 (1990) 357.
28. K. Eckhard, W. Schuhmann, *Analyst* 133 (2008) 1486.
29. J. Izquierdo, J.J. Santana, S. González, R.M. Souto, *Electrochim. Acta* 55 (2010) 8791.
30. P.M. Diakowski, A.S. Baranski, *Electrochim. Acta* 52 (2006) 854.
31. K. Eckhard, M. Etienne, A. Schulte, W. Schuhmann, *Electrochem. Commun.* 9 (2007) 1793.
32. K. Eckhard, T. Erichsen, M. Stratmann, W. Schuhmann, *Chem. Eur. J.* 14 (2008) 3968.
33. D. Ruhlig, W. Schuhmann, *Electroanalysis* 19 (2007) 191.
34. D. Ruhlig, H. Gugel, A. Schulte, W. Theisen, W. Schuhmann, *Analyst* 133 (2008) 1700.
35. J.J. Santana, M. Pähler, R.M. Souto, W. Schuhmann, *Electrochim. Acta* 77 (2012) 60.
36. M. Pähler, J. J. Santana, W. Schuhmann, R.M. Souto, *Chem. Eur. J.* 17 (2011) 905.
37. J.J. Santana, M. Pähler, W. Schuhmann, R.M. Souto, *ChemPlusChem* 77 (2012) 707.